FEBS Letters 588 (2014) 3291–3297

journal homepage: www.FEBSLetters.org

Structural features of peptoid–peptide hybrids in lipid–water interfaces

Lars Erik Uggerhøj [a], Jens K. Munk [b], Paul R. Hansen [b], Peter Güntert [c], Reinhard Wimmer [a,*]

[a] Department of Biotechnology, Chemistry, and Environmental Engineering, Aalborg University, Sohngaardsholmsvej 49, 9000 Aalborg, Denmark
[b] Department of Drug Design and Pharmacology, University of Copenhagen, Universitetsparken 2, 2100 Copenhagen, Denmark
[c] Institute of Biophysical Chemistry, Center for Biomolecular Magnetic Resonance, J. W. Goethe-University Frankfurt, Max-von-Laue-Str. 9, 60438 Frankfurt am Main, Germany

ARTICLE INFO

Article history:
Received 31 March 2014
Revised 24 June 2014
Accepted 14 July 2014
Available online 22 July 2014

Edited by Christian Griesinger

Keywords:
Antimicrobial peptides
Peptoids
NMR
Maculatin
Paramagnetic relaxation enhancement

ABSTRACT

The inclusion of peptoid monomers into antimicrobial peptides (AMPs) increases their proteolytic resistance, but introduces conformational flexibility (reduced hydrogen bonding ability and *cis*/*trans* isomerism). We here use NMR spectroscopy to answer how the insertion of a peptoid monomer influences the structure of a regular α-helical AMP upon interaction with a dodecyl phosphocholine (DPC) micelle. Insertion of [(2-methylpropyl)amino]acetic acid in maculatin-G15 shows that the structural change and conformational flexibility depends on the site of insertion. This is governed by the micelle interaction of the amphipathic helices flanking the peptoid monomer and the side chain properties of the peptoid and its preceding residue.
© 2014 Federation of European Biochemical Societies. Published by Elsevier B.V. All rights reserved.

1. Introduction

Antimicrobial peptides (AMPs) hold great potential as future antibiotics, as they show high antimicrobial activity against even multiresistant bacteria. However, AMPs are prone to proteolytic degradation and thus have short life times in the body. In order to increase proteolytic stability of AMPs, several peptidomimetics are researched. These include D-amino acids, peptoids, β-peptides, and hybrids hereof [1–6].

Single peptoid (N-substituted glycine [7]) residues in a peptide chain are conformationally flexible, as backbone hydrogen bonding is impossible due to the absence of H^N atoms, which are a major participant in stabilizing secondary structures. Furthermore, the *cis* and *trans* conformations can be equally favorable, causing the presence of both conformations [8].

Hybrids of peptides and peptoids are called "peptomers" [9] and examples of these have been found in nature, e.g. cyclosporine. (The term "peptomer" is, however, also used for polymers of peptides without any peptoid residues [10].) Artificial peptomers have been constructed as mimics of bacterial quorum sensing signals [11], synthetic inhibitors of a kinase [12], or as novel pharmaceuticals [13]. Lee and Zuckermann introduced peptoid residues into folded ribonuclease A and demonstrated that the resulting peptomer still retained some activity [14].

Peptoid residues were also successfully incorporated into AMPs: Incorporation of two alanine peptoid residues into the hydrophobic face of an α-helical AMP significantly reduced its hemolytic activity but not its antibacterial activity [15]. Substituting some of the leucine residues in the zipper motif of melittin with different peptoid residues resulted in helix disruption, but the antibacterial activity was still intact (while hemolysis was significantly reduced) [16]. Also hybrids with alternating peptide/peptoid building blocks were shown to have antimicrobial activity [3,17–19].

In this work, we investigate the effect of a single peptoid substitution on the structure of an α-helical AMP bound to a micelle. We have chosen maculatin as model AMP. Wild type maculatin 1.1, is a cationic 21 amino acid AMP (GLFGVLAKVAAHVVPAIAEHF-NH_2) extracted from the Australian frog *Litoria genimaculata* [20]. Maculatin exhibits antimicrobial activity against various microbial strains. It is unstructured in water, but in the presence of 50% trifluoroethanol (TFE) or dodecyl phosphocholine (DPC) micelles

Abbreviations: AMP, antimicrobial peptide; CCA, α-cyano-4-hydroxycinnamic acid; COSY, correlation spectroscopy; DIPCDI, diisopropylcarbodiimide; DPC, dodecyl phosphocholine; Fmoc, fluorenylmethyloxycarbonyl chloride; Gd(DTPA-BMA), gadolinium diethylenetriaminepentaacetic acid bismethylamide; HPLC, high pressure liquid chromatography; HSQC, heteronuclear single quantum coherence; Nleu, [(2-methylpropyl)amino]acetic acid; NOE, nuclear Overhauser effect; NOESY, nuclear Overhauser effect spectroscopy; PRE, paramagnetic relaxation enhancement; RMSD, root mean square deviation; SDS, sodium dodecyl sulfate; TFA, trifluoroacetic acid; TFE, trifluoroethanol; TIS, triisopropyl silane; TOCSY, total correlation spectroscopy

* Corresponding author. Fax: +45 98141808.
E-mail address: rw@bio.aau.dk (R. Wimmer).

http://dx.doi.org/10.1016/j.febslet.2014.07.016
0014-5793/© 2014 Federation of European Biochemical Societies. Published by Elsevier B.V. All rights reserved.

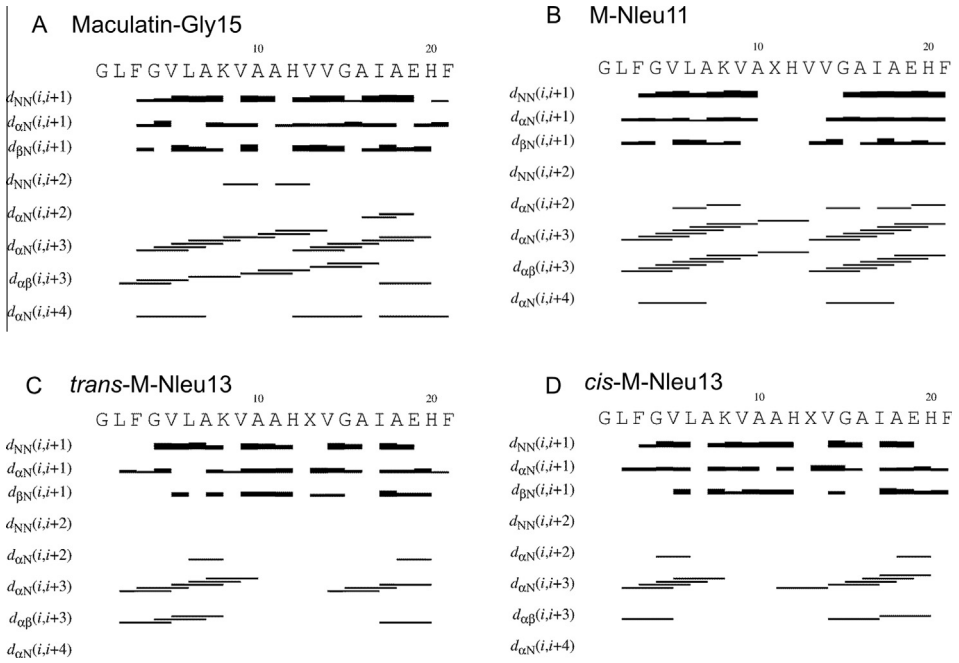

Fig. 1. Plots of sequential and medium-range NOEs vs. sequence visualizing secondary structure information contained in the NOESY spectra from different maculatin derivatives: (A) Maculatin-Gly15 in DPC micelles, (B) M-Nleu-11 in DPC micelles, (C) *trans*-M-Nleu-13 in SDS micelles, (D) *cis*-M-Nleu-13 in SDS micelles. "X" denotes the peptoid residue Nleu. In case of chemical shift degeneracy between atoms of M-Nleu-13 in the *cis* and *trans* conformers, the cross peaks were assumed to be present in both conformations.

it folds into an α-helix with a slight kink at Pro 15 [21]. Maculatin-G15 (P15G mutation) [22] was found to fold into a complete α-helix in the presence of DPC micelles (Fig. 1A). We use the continuous α-helix in maculatin-G15 as the scaffold for studying both the local and global structural consequences of inserting a peptoid monomer into a regular α-helical AMP. As model peptoid residue, we chose Nleu, [(2-methylpropyl)amino]acetic acid (Fig. S1), as its side chain is identical to that of leucine, a very frequent amino acid in AMPs.

2. Materials and methods

2.1. Materials

All standard fluorenylmethyloxycarbonyl chloride (Fmoc) protected amino acids, 99.5% Isobutylamine, 99% bromoacetic acid, trifluoroacetic acid (TFA), and triisopropyl silane (TIS), were purchased from Fluka. Piperidine and N,N′-Diisopropylcarbodiimide (DIPCDI) from Iris Biotech. α-cyano-4-hydroxycinnamic acid (CCA) from Bruker Daltonics. DPC and sodium dodecyl sulfate (SDS) from Avanti Polar Lipids and DPC-d_{38} (98% D) and SDS-d_{25} (98% D) from Cambridge Isotope Laboratories, and the remaining chemicals were purchased from Sigma–Aldrich.

2.2. Peptide synthesis

Peptomers were synthesized using Fmoc solid phase peptide synthesis and the submonomer approach [23,24], purified by high pressure liquid chromatography (HPLC), and verified by mass spectroscopy as described before [3].

2.3. Calculation of expected short distances

Starting from the structures of *cis* and *trans*-maculatin-Nleu11, respectively, distances between atoms of interest were calculated while systematically varying one or two dihedral angles. Dihedral angles were defined as following with Nleu as residue *i*:

φ_i: C_{i-1}-N_i-$C^{\alpha}{}_i$-C'_i, ψ_i: N_i-$C^{\alpha}{}_i$-C'_i-N_{i+1}. In the case of Nleu, χ_1 was defined as C_{i-1}-N_i-$C^{\beta}{}_i$-$C^{\gamma}{}_i$.

2.4. NMR spectroscopy

Each peptide was dissolved to 3 mM in 10 mM phosphate buffer, pH 6.5, containing 5% D_2O, 2 mM NaN_3 and, 150 mM DPC-d_{38} or SDS-d_{25}.

Spectra were recorded on Bruker DRX600 spectrometers at 37 °C. Additional spectra measured at 20 °C were used for resolving overlapping spin systems. TopSpin v. 1.3 and 2.1 were used for recording processing NMR data. The following spectra were recorded: ^{1}H-^{1}H-TOCSY (75 ms mixing time), ^{1}H-^{1}H-NOESY (60 ms mixing time), ^{1}H-^{1}H-COSY and ^{1}H-^{13}C-HSQC (natural abundance). Excitation sculpting [25] was used for water suppression in homonuclear 2D-spectra.

The individual spin systems were assigned in the ^{1}H-^{1}H-TOCSY spectra using CARA v. 1.8.4 with the aid of the ^{1}H-^{13}C-HSQC, ^{1}H-^{1}H-COSY, and ^{1}H-^{1}H-NOESY spectra. Subsequently, integration of NOESY cross peaks were performed in the NEASY subroutine of CARA v. 1.5.5 [26]. C^{α} and C^{β} chemical shifts were obtained from the ^{1}H-^{13}C-HSQC spectra and used to calculate backbone torsion angle restrains using the program TALOS+ [27]. The peptoid residue itself and the residues preceding and succeeding the peptoid residue, were excluded from TALOS+ analysis.

2.5. PRE constraints

Paramagnetic relaxation enhancement (PRE) constraints were derived as described by Franzmann et al. [28]. Eight inversion recovery nuclear Overhauser effect spectroscopy (NOESY) spectra with recovery delay times of 1, 50, 150, 400, 700, 1200, 2600, and 4000 ms were recorded in a pseudo-3D manner for each of the four gadolinium diethylenetriaminepentaacetic acid bismethylamide (Gd(DTPA-BMA)) titration points: 0, 2, 5, 10 mM. All peaks with H^{α} in the indirect dimension were integrated in all spectra. R_1 relaxation rates were determined, and by a linear fit of the

relaxation rates for the 4 titration points the PRE values were determined. PRE values for each H^{α} were then converted to distance restraints to the micelle center as described [28]: If there was more than one PRE value for a given H^{α}, we used the average value of obtained distances. For H^{α} yielding three or more PREs, we also calculated the standard deviation of the distances. Standard deviations for the PRE derived distances were between 0.1 and 1.0 Å. Thus, all PRE derived distances were used as upper and lower distance restraints with values of average distance ±1 Å, respectively, also for atoms yielding less than three PREs, not permitting the calculation of standard deviations. PRE-derived distance restraints were weighted with 10% compared to the NOE-derived distance restraints [28].

2.6. Structure calculation

A pseudoatom representing the micelle center was attached to the C-terminal end of the peptide by a ≈70 Å flexible linker consisting of pseudoatoms (CYANA residues -LL-LL2-LL2-$(LL5)_{11}$-$(LL2)_4$-LL-). On the basis of the NOE-derived distance constraints, angle restraints and PRE-derived distance restraints, 80 structures of each peptide were calculated using CYANA v. 2.1 [29]. The 20 structures with the lowest target function value were included in the final structure ensemble. For overlapping NOE peaks between the *cis* and *trans* conformer, 90% of the total peak intensity was used. The resulting integral values were then split according to the ratio of 1.3 between the *trans* and *cis* conformer. This ratio was found as an average based on the peak intensities of completely resolved peaks in the total correlation spectroscopy (TOCSY) spectra.

3. Results

It is advantageous for the structure calculation of a peptomer that the conformation of the peptoid monomer (*cis* or *trans*) is determined to start with.

Cis and *trans* conformations each show characteristic short distances: the distance between $H^{N}_{(i-1)}$ and H^{α}_{i} (with *i* denoting the peptoid residue) is in the *trans* conformation bigger than 3.6 Å, while this distance in the *cis* conformation can be <2.5 Å, depending on

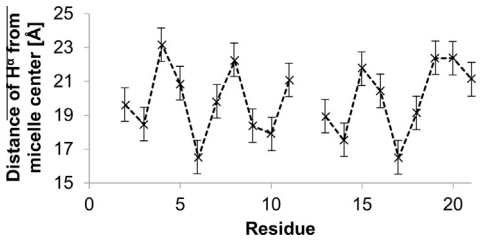

Fig. 3. Distance from the micelle center to H^{α} atoms of M-Nleu11 in DPC micelles obtained from PRE experiments. For structure calculations, these values were used as distance restraints with ±1 Å and a weight of 10% relative to NOE distance restraints.

$\psi_{(i-1)}$. Independent of $\varphi_{(i-1)}$ and $\psi_{(i-1)}$, this distance will always be shorter in the *cis* than in the *trans* conformation. This behavior is opposite for the distance between $H^{N}_{(i-1)}$ and H^{β}_{i}. Likewise, the distances between $H^{\alpha}_{(i-1)}$ and $H^{\alpha 2,3}{}_{i}$ are shorter in the *cis* conformation, while the distances $H^{\alpha}{}_{(i-1)}$ and $H^{\beta 2,3}{}_{i}$ are shorter in the *trans* conformation (Fig. S2).

The sequences of the two maculatin-G15 analogs investigated in this study are:

M-Nleu11 GLFGVLAKVA-Nleu-HVVGAIAEHF-NH_2

M-Nleu13 GLFGVLAKVAAH-Nleu-VGAIAEHF-NH_2

M-Nleu11 showed only one conformer when bound to SDS or DPC micelles and was found to have a *trans* conformation of the Nleu residue based on the NOESY cross peaks from H^{α} Ala10 to H^{β} Nleu11 (Fig. 2). The insertion of the molecule into the DPC micelle was determined by paramagnetic relaxation enhancement (PRE) experiments. These data are shown in Fig. 3 and were used as restraints for the structure calculations.

M-Nleu13 exhibited an almost equal distribution between *cis* and *trans* isomers of Nleu, and both structures were solved bound to SDS micelles. Useful PRE data could not be obtained for this analog, because of H^{α} chemical shift degeneracy between the two conformations.

NMR assignments and structure ensembles of M-Nleu11 in DPC micelles and M-Nleu13 (*cis* and *trans*) in SDS micelles have been submitted to the PDB and BMRB databases. The structural statistics and accession codes are given in Table 1.

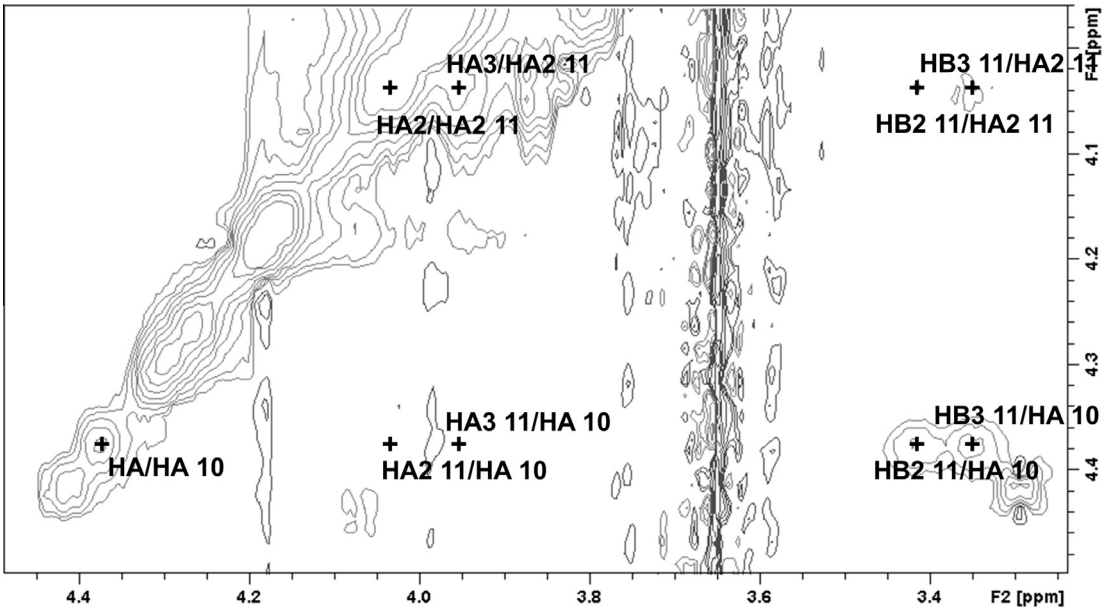

Fig. 2. Region of a NOESY spectrum of M-Nleu11 in DPC micelles containing the NOEs for distinguishing *cis* and *trans* peptoid conformation. It shows the absence of $H^{\alpha}_{(i-1)}$–$H^{\alpha}_{(i)}$ NOEs and the presence of the $H^{\alpha}_{(i-1)}$–$H^{\beta}_{(i)}$ NOEs (with *i* denoting the peptoid residue). The NOESY section also shows weak cross peaks between $H^{\alpha 2}$ and $H^{\beta 2/3}$ of Nleu 11.

Table 1
Structural statistics for the NMR structure ensembles of M-Nleu11 and M-Nleu13.

Peptomer	M-Nleu11	M-Nleu13	M-Nleu13
Nleu conformation	*Trans*	*Trans*	*Cis*
Database entries	PDB: 2MMJ BMRB: 19856	PDB: 2MN9 BMRB: 19883	PDB: 2MN8 BMRB: 19882
Number of distance restraints			
Intra-residue	80	80	80
Sequential ($\|i-j\|=1$)	69	51	51
Medium-range ($1<\|i-j\|<5$)	56	24	24
To micelle center	19	–	–
TALOS + derived dihedral angle restraints[a]			
φ angles	15	16	16
Ψ angles	15	16	16
CYANA residual target function value (Å^2)	0.31 ± 0.02	0.06 ± 0.01	0.12 ± 0.04
RMSD for residue 2–21			
Average backbone (N, C$^\alpha$, C′)	0.20 ± 0.04	2.11 ± 0.50	1.98 ± 0.40
Average heavy atoms	0.57 ± 0.07	3.10 ± 0.64	3.18 ± 0.70
RMSD for region preceding Nleu	Residues 2–9	Residues 2–10	Residues 2–10
Average backbone (N, C$^\alpha$, C′)	0.04 ± 0.01	0.35 ± 0.09	0.39 ± 0.11
Average heavy atoms	0.50 ± 0.09	0.77 ± 0.13	0.80 ± 0.18
RMSD for region following Nleu	Residues 12–21	Residues 14–21	Residues 14–21
Average backbone (N, C$^\alpha$, C)	0.11 ± 0.03	0.28 ± 0.09	0.32 ± 0.13
Average heavy atoms	0.51 ± 0.09	0.73 ± 0.10	0.73 ± 0.15
Restraint violations			
No of NOE restraint violations > 0.1 Å	0	0	0
Maximum NOE violation	0.1	0.1	0.1
No of dihedral angle restraint violations > 5°	0	0	0
Maximum PRE restraint violation	0.58 Å	–	–
Ramachandran plot statistics[a]			
Residues in favored regions	86.8%	98.9%	97.5%
Residues in additional allowed regions	13.2%	1.1%	2.5%
Residues in generously allowed regions	0.0%	0.0%	0.0%
Residues in disallowed regions	0.0%	0.0%	0.0%

[a] The peptoid residue and the residues preceding and succeeding it were excluded from analysis.

Analysis of NOE patterns show that all three structures showed a well-defined α-helix in both ends of the molecule, with a flexible region around the Nleu residue (Fig. 1).

It was possible to obtain insertion depth data for M-Nleu11 in DPC, which determined the orientation of the two terminal α-helices relative to each other. The structure ensemble resulting from the use of PRE derived restraints is rigid around the peptoid residue, yielding lower average backbone root mean square deviation (RMSD) for M-Nleu11 than for M-Nleu13. The final structure ensemble of M-Nleu11 is shown in Fig. 4C. Its hydrophobic residues are oriented towards the micelle center, the polar and Gly residues are oriented towards the lipid head groups and solvent surrounding the micelle (except for His20), and the Ala residues are primarily located in an orientation parallel with the micelle surface (Fig. 5A).

In order to understand why one of the maculatin analogs is found in only one conformation while the other has two conformations, the hypothetical structure of M-Nleu11 with *cis*-Nleu was calculated using all experimental data, but forcing Nleu 11 into the *cis* conformation. Fig. 5 shows the orientation of the Nleu side chain in the *trans* and the hypothetical *cis* conformation. In the *trans* conformation, the side chain is buried in the micelle, and in the hypothetical *cis* conformation, the side chain would be exposed to the bulk water.

4. Discussion

4.1. Distinguishing between cis and trans conformation

Initially, we attempted to solve the structures of both maculatin analogs in a solution of SDS. However, due to identical chemical shifts of H$^\alpha$ Ala10 and H$^\beta$ Nleu11 in M-Nleu11 bound to SDS, the presence of NOESY cross peaks between these atoms could not be established. Thus, a M-Nleu11 sample using DPC as the membrane mimic was used, where these peaks were resolved. In this sample, NOESY cross peaks from H$^\alpha$ Ala10 to the side chain of Nleu11 were present (see Fig. 2), thus establishing that this analog contains a *trans* peptoid bond. The presence of a smaller amount of *cis* conformation cannot be ruled out completely, but additional spin systems were not present. Based on the signal-to-noise ratio of the strongest signals in the NOESY spectrum, we estimate that an eventually present *cis* conformation would be populated to less than 5%. When calculating the structure of M-Nleu11 in both the *trans* and *cis* conformation, the distance restraints from H$^\alpha$ Ala10 to the Nleu11 side chain were the only ones that could not be fulfilled by both conformations. Very recently, a computational study of conformational preferences of peptomers was published, investigating the optimum backbone dihedral angles of an alanine residue preceding a peptoid residue (N-methyl-glycine) [30]. The optimum angles are found within the regions adopted by pre-proline residues in the PDB database from the "Richardson top 8000" database [31]. Fig. 6 shows the ϕ/ψ angle distribution of the amino acid preceding the peptoid residue in the structures presented here. While the ϕ/ψ angles of Ala 10 in *trans*-M-Nleu-11 are close to what can be expected for an amino acid preceding a peptoid, they do not fit for *cis*-M-Nleu-11, further substantiating the presence of a *trans* conformation.

In M-Nleu13, one of the conformers was found to have a NOESY cross peak from H$^\alpha$ His12 to the Nleu13 side chain, thus being the *trans* conformer. The other conformer had weak NOESY cross peaks from H$^\alpha$ His12 to H$^\alpha$ Nleu13 (i.e. backbone to backbone), which should only be found in the *cis* conformer.

4.2. Structural evaluation

For both M-Nleu11 and M-Nleu13, the insertion of the peptoid monomer exerts a helix breaking effect. From the NOESY spectra this can be seen directly due to very weak or missing H$^\alpha(i)$–H$^N(i+3)$ NOESY cross peaks across the Nleu residue

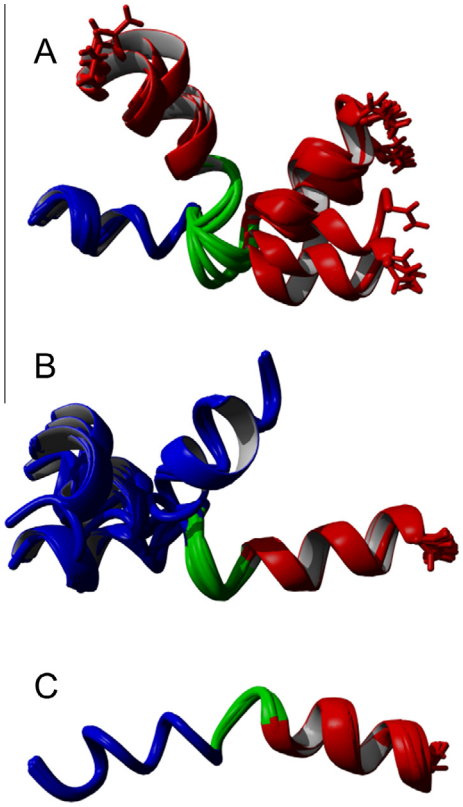

Fig. 4. Structure ensembles of M-Nleu11 in DPC micelles with Nleu in the *trans* conformation. (A) Superposition of residues 2–10 calculated without PRE restraints. (B) Superposition of residues 12–21 calculated without PRE restraints. (C) Superposition of residues 2–21 calculated with PRE restraints. Residues 1–9 are colored blue, residues 10–12 are colored green, and residues 13–21 plus the C-terminal amide are colored red. The image was generated using the POVRay plugin to YASARA [33].

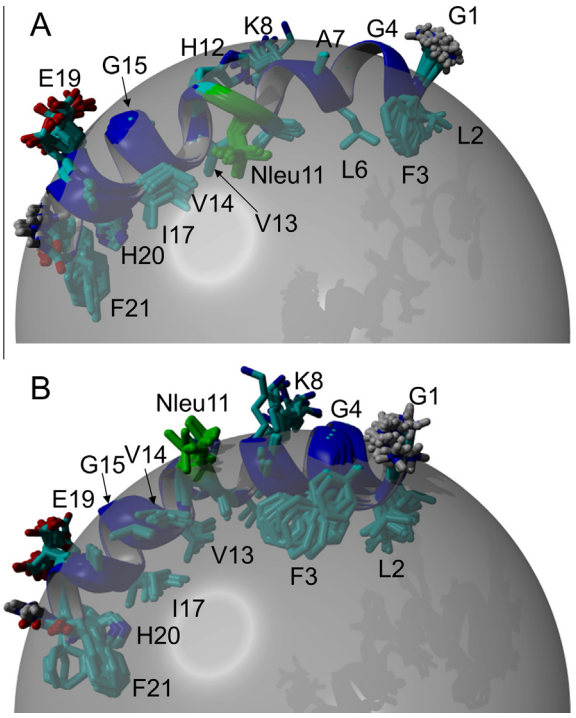

Fig. 5. Comparison of M-Nleu11 *trans* (panel A, actual structure) and *cis* (panel B, hypothetical structure) in DPC micelles. Only the *trans* conformation was observed experimentally, the *cis* conformation was calculated by forcing ω_{Nleu11} to 0°, otherwise the same restraints were used. The micelle is indicated by a semi-transparent grey sphere with a radius of 22.7 Å. Both in the *trans* and the *cis*-structure, the charges at the N-terminus, Lys 8 and E19, are located at the micelle-water interface. So are the uncharged C-terminal amide and His 12, while His 20 is immersed deeper into the micelle. Other residues at the micelle surface include Gly 4, Ala 7 and Gly 15. The hydrophobic residues (Phe, Leu, Val, Ile) point towards the hydrophobic interior of the micelle. The peptoid residue, shown in green, points towards the solvent in the *cis*-conformation, but towards the micelle interior in the *trans* conformation. The figure was created with YASARA [33].

(Fig. 1). Furthermore, the helix breaking effect is clearly visible from the structure ensembles of both analogs (without PRE-derived restraints), as they are characterized by well-defined helices at both termini with a very flexible region around the Nleu residue. The helix breaking effect is likely due to the steric repulsion between the Nleu side chain and the side chain of the previous residue as well as the loss of the hydrogen bonding H^N atom.

After inclusion of the PRE-derived restraints for M-Nleu11, the RMSD for the structure ensemble becomes quite low. Despite the lack of regular secondary structure around the peptoid residue, the position of the two terminal helices relative to each other is well defined as a consequence of the restraints to the micelle center. In α-helical cationic AMPs, the peptides fold into an amphipathic structure where the hydrophobic residues are inserted into the membrane interior and the polar residues are interacting with the lipid head groups and the surrounding solvent [28,32]. Therefore, the 20 structures of M-Nleu11 become very similar: the two helical ends of the molecule insert into the membrane mimic and lock the otherwise flexible region in place. This demonstrates the usefulness of PRE experiments to determine the insertion depth of each residue. Without this information, it is not possible to determine the orientation of the two helical ends of the molecule relative to each other (Fig. 4, panel A and B).

The structures of M-Nleu13 were solved without the use of PRE-derived restraints. The high degree of similarity of chemical shifts between the two conformers and resulting overlap of peaks made it impossible to obtain distinguishable relaxation rates. The lack of insertion depth data allows for highly variable orientations of the two helices relative to each other (Fig. 7). Thus, only the fact that

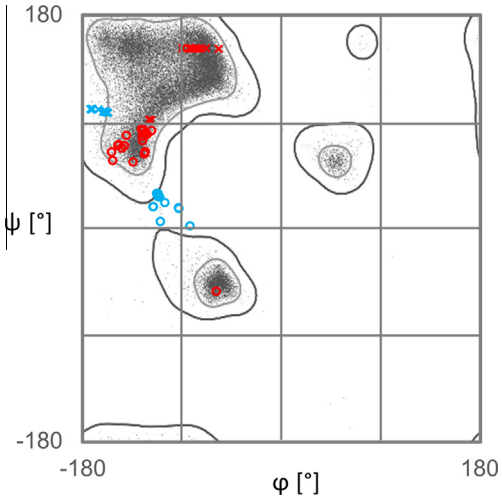

Fig. 6. Ramachandran plot showing the distribution of the backbone torsion angles of the amino acid preceding the peptoid residue in maculatin-based peptomers: Ala 10 in M-Nleu-11 (blue) and His 12 in M-Nleu-13 (red). Circles denote *cis* conformation of the peptoid, crosses denote *trans* conformation of the peptoid. The black and white background shows the distribution of ϕ/ψ angles in amino acid residues preceding proline according to "Richardon's top 8000" database [31]. The data show that His 12 of both *cis* and *trans* conformations of M-Nleu-13 is located in the favorable regions of the energy landscape. Conversely, Ala 10 in M-Nleu-11 is only located close to a favorable region in the *trans*, but not the *cis* conformation of the succeeding peptoid.

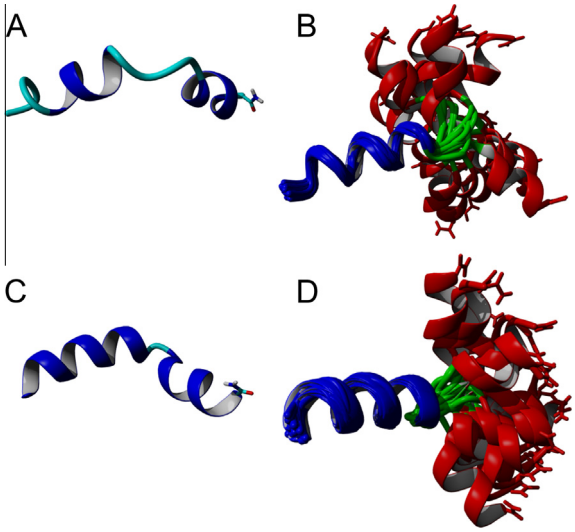

Fig. 7. Structure ensembles of M-Nleu13 illustrating how the peptide folds into two α-helices for both the *trans* (A and B) and *cis* (C and D) conformation of Nleu13, as well as how flexible the middle region around the Nleu residue is. In panels A and C, the backbone structure of a single conformer from the bundle is displayed to illustrate the helical structure. Residues in blue are classified by YASARA [33] as helical whereas residues in cyan are not. In panels B and D, the entire bundle of 20 conformers is displayed as a superposition of residues 2–10. Residues 1–11 are colored blue, residues 12–14 are colored green, and residues 15–21 plus the C-terminal amide are colored red.

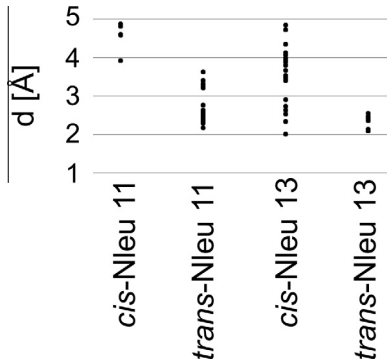

Fig. 8. Shortest distance found between any two hydrogen atoms of the peptoid side chain and the preceding peptide side chain in all 20 calculated structures of both peptomers studied in their *cis* and *trans* conformations. The Van der Waals radius of hydrogen is 1.2 Å, thus making distances closer than 2.4 Å energetically unfavorable.

both ends fold into a helical structure, and that this molecule has an almost equal tendency to adopt a *trans* and *cis* conformation can be concluded.

4.3. Why is the trans conformation preferred in M-Nleu11?

In the two maculatin analogs presented here, the Nleu residue was inserted at two different positions. One of these positions yields a molecule which prefers only a *trans* conformation of the Nleu residue, whereas the other has an equal tendency to adopt both *cis* and *trans* conformations of the Nleu residue.

In the well-defined structures of M-Nleu11, a closer look on the Nleu residue shows that the side chain properties as well as the place of insertion of the peptoid monomer might be the determining factors for preferring the *trans* conformation:

In M-Nleu11, the orientation of the peptide on the micelle-water interface is determined by the amphipathicity of the two helical segments. They will orient on the micelle surface such as is most favorable for them. Under these conditions, the Nleu side chain will be oriented towards the solvent in the *cis* conformation but towards the membrane interior in the *trans* conformation, as shown in Fig. 5. This difference in orientation might explain why only the *trans* conformation is found for this peptide.

4.4. Why are both cis and trans conformation present in M-Nleu13

By following the argumentation for M-Nleu11, the reason why the *cis* and *trans* conformations are present in almost equimolar amounts in M-Nleu13 is that both conformations achieve an energetically equally favorable structure upon interaction with the membrane mimic.

The Nleu side chain is located on the opposite side of the helix in M-Nleu13, where the backbone of the residue in wild-type maculatin (Val) is inserted into the hydrophobic interior of the micelle. It is possible that both the *cis* and *trans* conformation allows for the hydrophobic Nleu side chain to be inserted into the hydrophobic interior of the micelle, but we cannot conclude on this based on structures without PRE-derived constraints. In addition, Nleu-13 follows the bulky His-12, while Nleu-11 follows the less bulky Ala-10. Distances between side chain atoms of a peptoid and the side chain atoms of its preceding residue are generally shorter for the *trans* conformer. Fig. 8 shows the distribution of shortest inter-sidechain distances in all 20 structures of all four molecules calculated. *Trans*-M-Nleu-13 shows distances <2.4 Å (twice the VdW radius of hydrogen), leading to steric clashes, while *cis*-M-Nleu-13 displayed a wide range of distances both favorable and unfavorable. This might also be a reason for this molecule to partly adopt a *cis* conformation. Very short distances are also present in *trans*-M-Nleu-11, but to a lesser extent.

5. Conclusion

The insertion of a peptoid monomer into an α-helical AMP disrupts the helix. Inserting the Nleu residue can result in both a *cis* and *trans* conformation of the peptide. The conformations can be determined experimentally by the presence of NOESY cross peaks from H^{α} of the preceding residue to either the side chain H^{β} (*trans*) or backbone H^{α} (*cis*) of the peptoid residue. As the side chain of the peptoid monomer is shifted counter-clockwise in the helical wheel, hydrophobic peptoid monomers should be placed on the left-handed side of the helical wheel (looking down the helical axis from the N-to the C-terminus, with the helix oriented such that the membrane interior points downwards) near the middle of maculatin in order for only the *trans* conformer to be present. When inserting Nleu on the right-handed side of the helical wheel near the middle of an AMP, both the *cis* and *trans* conformers can be present. In addition, *trans* conformers can be favored by not placing the peptoid after a bulky residue, as bulky residues favor the *cis* conformation in subsequent peptoids. Furthermore, we have demonstrated the usefulness of PRE experiments for determining the global structure of peptomers bound to micelles.

Acknowledgements

This project was conducted in the framework of the Danish Center for Antibiotic Research and Development (DanCARD) financed by The Danish Council for Strategic Research (Grant No. 09-067075). We thank the Centre for Biomolecular Magnetic Resonance, Frankfurt, Germany, for access to NMR equipment and Dr. Frank Löhr for expert assistance. The sequence plots of Maculatin-Gly15 were provided by Magnus Franzmann and Kirstine Nielsen. The NMR laboratory at Aalborg University is supported by the Obel, SparNord and Carlsberg Foundations.

Appendix A. Supplementary data

Supplementary data associated with this article can be found, in the online version, at http://dx.doi.org/10.1016/j.febslet.2014.07.016.

References

[1] Miller, S.M., Simon, R.J., Ng, S., Zuckermann, R.N., Kerr, J.M. and Moos, W.H. (1994) Proteolytic studies of homologous peptide and N-substituted glycine peptoid oligomers. Bioorg. Med. Chem. Lett. 4, 2657–2662.

[2] Godballe, T., Nilsson, L.L., Petersen, P.D. and Jenssen, H. (2011) Antimicrobial β-peptides and α-peptoids. Chem. Biol. Drug Des. 77, 107–116.

[3] Meinike, K. and Hansen, P.R. (2009) Peptoid analogues of anoplin show antibacterial activity. Protein Pept. Lett. 16, 1006–1011.

[4] Pripotnev, S., Won, A. and Ianoul, A. (2010) The effects of L- to D-isomerization and C-terminus deamidation on the secondary structure of antimicrobial peptide Anoplin in aqueous and membrane mimicking environment. J. Raman Spectrosc. 41, 1645–1649.

[5] Olsen, C.A., Bonke, G., Vedel, L., Adsersen, A., Witt, M., Franzyk, H. and Jaroszewski, J.W. (2007) Alpha-peptide/beta-peptoid chimeras. Org. Lett. 9, 1549–1552.

[6] Chongsiriwatana, N.P., Patch, J.A., Czyzewski, A.M., Dohm, M.T., Ivankin, A., Gidalevitz, D., Zuckermann, R.N. and Barron, A.E. (2008) Peptoids that mimic the structure, function, and mechanism of helical antimicrobial peptides. Proc. Natl. Acad. Sci. USA 105, 2794–2799.

[7] Simon, R.J., Kania, R.S., Zuckermann, R.N., Huebner, V.D., Jewell, D.A., Banville, S., Ng, S., Wang, L., Rosenberg, S., Marlowe, C.K., Spellmeyer, D.C., Tan, R.Y., Frankel, A.D., Cohen, F.E., Santi, D.V. and Bartlett, P.A. (1992) Peptoids: a modular approach to drug discovery. Proc. Natl. Acad. Sci. 89, 9367–9371.

[8] Moure, A., Sanclimens, G., Bujons, J., Masip, I., Alvarez-Larena, A., Pérez-Payá, E., Alfonso, I. and Messeguer, A. (2011) Chemical modulation of peptoids: synthesis and conformational studies on partially constrained derivatives. Chem. Eur. J. 17, 7927–7939.

[9] Ostergaard, S. and Holm, A. (1997) Peptomers: a versatile approach for the preparation of diverse combinatorial peptidomimetic bead libraries. Mol. Divers. 3, 17–27.

[10] Robey, F.A., Kelson-Harris, T., Roller, P.P. and Robert-Guroff, M. (1995) A helical epitope in the C4 domain of HIV glycoprotein 120. J. Biol. Chem. 270, 23918–23921.

[11] Fowler, S.A., Stacy, D.M. and Blackwell, H.E. (2008) Design and synthesis of macrocyclic peptomers as mimics of a quorum sensing signal from *Staphylococcus aureus*. Org. Lett. 10, 2329–2332.

[12] Murugan, R.N., Park, J.-E., Lim, D., Ahn, M., Cheong, C., Kwon, T., Nam, K.-Y., Choi, S.H., Kim, B.Y., Yoon, D.-Y., Yaffe, M.B., Yu, D.Y., Lee, K.S. and Bang, J.K. (2013) Development of cyclic peptomer inhibitors targeting the polo-box domain of polo-like kinase 1. Bioorg. Med. Chem. 21, 2623–2634.

[13] Ovadia, O., Linde, Y., Haskell-Luevano, C., Dirain, M.L., Sheynis, T., Jelinek, R., Gilon, C. and Hoffman, A. (2010) The effect of backbone cyclization on PK/PD properties of bioactive peptide–peptoid hybrids: the melanocortin agonist paradigm. Bioorg. Med. Chem. 18, 580–589.

[14] Lee, B.-C. and Zuckermann, R.N. (2011) Protein side-chain translocation mutagenesis via incorporation of peptoid residues. ACS Chem. Biol. 6, 1367–1374.

[15] Song, Y.M., Park, Y., Lim, S.S., Yang, S.-T., Woo, E.-R., Park, I.-S., Lee, J.S., Kim, J.I., Hahm, K.-S., Kim, Y. and Shin, S.Y. (2005) Cell selectivity and mechanism of action of antimicrobial model peptides containing peptoid residues. Biochemistry 44, 12094–12106.

[16] Zhu, W.L., Song, Y.M., Park, Y., Park, K.H., Yang, S.-T., Kim, J.I., Park, I.-S., Hahm, K.-S. and Shin, S.Y. (2007) Substitution of the leucine zipper sequence in melittin with peptoid residues affects self-association, cell selectivity, and mode of action. Biochim. Biophys. Acta 1768, 1506–1517.

[17] Patch, J.A. and Barron, A.E. (2003) Helical peptoid mimics of magainin-2 amide. J. Am. Chem. Soc. 125, 12092–12093.

[18] Ryge, T.S., Frimodt-Moller, N. and Hansen, P.R. (2008) Antimicrobial activities of twenty lysine-peptoid hybrids against clinically relevant bacteria and fungi. Chemotherapy 54, 152–156.

[19] Ryge, T.S. and Hansen, P.R. (2006) Potent antibacterial lysine-peptoid hybrids identified from a positional scanning combinatorial library. Bioorg. Med. Chem. 14, 4444–4451.

[20] Rozek, T., Waugh, R.J., Steinborner, S.T., Bowie, J.H., Tyler, M.J. and Wallace, J.C. (1998) The Maculatin peptides from the skin glands of the tree frog *Litoria genimaculata*: a comparison of the structures and antibacterial activities of Maculatin 1.1 and Caerin 1.1. J. Pept. Sci. 4, 111–115.

[21] Chia, B.C., Carver, J.A., Mulhern, T.D. and Bowie, J.H. (2000) Maculatin 1.1, an anti-microbial peptide from the Australian tree frog, *Litoria genimaculata* solution structure and biological activity. Eur. J. Biochem. 267, 1894–1908.

[22] Ambroggio, E.E., Separovic, F., Bowie, J.H., Fidelio, G.D. and Bagatolli, L.A. (2005) Direct visualization of membrane leakage induced by the antibiotic peptides: maculatin, citropin, and aurein. Biophys. J. 89, 1874–1881.

[23] Zuckermann, R.N., Kerr, J.M., Kent, S.B.H. and Moos, W.H. (1992) Efficient method for the preparation of peptoids [oligo(N-substituted glycines)] by submonomer solid-phase synthesis. J. Am. Chem. Soc. 114, 10646–10647.

[24] Chann, W.C. and White, P.D. (2000) Fmoc Solid Phase Peptide Synthesis: A Practical Approach, Oxford Univ. Press.

[25] Hwang, T.L. and Shaka, A.J. (1995) Water suppression that works. Excitation sculpting using arbitrary wave-forms and pulsed-field gradients. J. Magn. Reson. Ser. A 112, 275–279.

[26] Keller, R. (2004) The Computer Aided Resonance Assignment Tutorial, first ed, CANTINA Verlag, Goldau (Switzerland).

[27] Shen, Y., Delaglio, F., Cornilescu, G. and Bax, A. (2009) TALOS+: a hybrid method for predicting protein backbone torsion angles from NMR chemical shifts. J. Biomol. NMR 44, 213–223.

[28] Franzmann, M., Otzen, D. and Wimmer, R. (2009) Quantitative use of paramagnetic relaxation enhancements for determining orientations and insertion depths of peptides in micelles. ChemBioChem 10, 2339–2347.

[29] López-Méndez, B. and Güntert, P. (2006) Automated protein structure determination from NMR spectra. J. Am. Chem. Soc. 128, 13112–13122.

[30] G.L. Butterfoss, K. Drew, P.D. Renfrew, K. Kirshenbaum, R. Bonneau, Conformational preferences of peptide–peptoid hybrid oligomers, Biopolymers (2014) in press, http://dx.doi.org/10.1002/bip.22516.

[31] Richardson, J.S., Keedy, D.A. and Richardson, D.C. (2013) "The plot" thickens: more data, more dimensions, more uses in: Biomolecular Forms and Functions. A Celebration of 50 Years of the Ramachandran Map (Bansal, M. and Srinivasan, N., Eds.), pp. 46–61, World Scientific, Singapore (ISBN: 978-981-4449-13-7).

[32] Vad, B., Thomsen, L.A., Bertelsen, K., Franzmann, M., Pedersen, J.M., Nielsen, S.B., Vosegaard, T., Valnickova, Z., Skrydstrup, T., Enghild, J.J., Wimmer, R., Nielsen, N.C. and Otzen, D.E. (2010) Divorcing folding from function: how acylation affects the membrane-perturbing properties of an antimicrobial peptide. Biochim. Biophys. Acta Proteins Proteomics 1804, 806–820.

[33] Krieger, E., Koraimann, G. and Vriend, G. (2002) Increasing the precision of comparative models with YASARA NOVA-a self-parameterizing force field. Proteins 47, 393–402.